Irrigation Science (2022) 40:45–54
https://doi.org/10.1007/s00271-021-00758-8

TECHNICAL BRIEF

Evaluating a novel microtensiometer for continuous trunk water potential measurements in field-grown irrigated grapevines

Vinay Pagay[1]

Received: 24 June 2021 / Accepted: 8 October 2021 / Published online: 12 November 2021

Abstract

Water potential (Ψ_w) is a fundamental thermodynamic parameter that describes the activity of water and is a key metric of plant water status. In this paper, we evaluate the continuous measurement of water potential in grapevine trunks using a novel in situ sensor known as a 'microtensiometer' under field conditions in two South Australian vineyards. We characterised the seasonal and diurnal dynamics of trunk water potentials (Ψ_{trunk}) obtained from microtensiometers installed in two grapevine cultivars, Shiraz and Cabernet Sauvignon, and compared these values to pressure chamber-derived stem (Ψ_{stem}) and leaf (Ψ_{leaf}) water potentials. Diurnal patterns of Ψ_{trunk} matched those of Ψ_{stem} and Ψ_{leaf} under low-vapour pressure deficit (VPD) conditions, but diverged under high-VPD conditions, where Ψ_{trunk} dropped below Ψ_{stem} in the late afternoon. Interestingly, under high-VPD conditions, Ψ_{trunk} values consistently dropped below Ψ_{stem} values around mid-afternoon with a recovery observed by early evening. The highest diurnal values of Ψ_{trunk} were observed shortly after dawn. Ψ_{stem} was better correlated with Ψ_{trunk} than was Ψ_{leaf} in both cultivars. Time cross-correlation analysis revealed that Shiraz Ψ_{trunk} lagged Cabernet Ψ_{trunk} in response to changing VPD. Microtensiometer-derived Ψ_{trunk} generally matched the seasonal and diurnal patterns of plant Ψ_w obtained with a pressure chamber except under high-VPD conditions. To be useful for irrigation scheduling, where absolute values of Ψ_w are required, crop- and cultivar-specific thresholds of Ψ_{trunk} need to be developed.

Introduction

Measurements of crop water status, which are essential for optimised irrigation scheduling, have historically relied on low throughput and high cost instruments, and labour intensive methods, that have decreased their utility and uptake by the farming community. One such method widely established to reliably quantify plant water status is the manual measurement of leaf or stem water potential (Shackel 2011; Williams and Baeza 2007), using a Scholander pressure chamber invented in the 1960s (Scholander et al. 1965). To overcome some of the limitations of such manual techniques, several electronic plant-based sensors to continuously measure crop water status have recently been developed that are based on various sensing modalities. These include sap flow sensors (Ginestar et al. 1998), thermal diffusivity sensors (Pagay and Skinner 2018), dendrometers (Corell et al. 2014), and thermal or infrared sensors (Jones 1999). A recent review of several of these sensors as applied in tree fruit crops can be found in Scalisi et al. (2017).

Given the prevalence of water potential as a reliable crop water status metric, sensors to measure plant water potential have also been developed. These sensors, known as hygrometers or psychrometers, provide continuous measurements of water potential either as contact sensors on leaves or in situ sensors embedded in stems (Dixon and Tyree 1984; McBurney and Costigan 1984; Michel 1977). Hygrometers measure the water potential of the vapour phase. They are prone to significant errors due to the requirement of isothermal conditions between the measurement junction and plant tissue (Dixon and Tyree 1984). A 1 °K temperature difference between the plant tissue and sensor can result in a water potential error of over 7.7 MPa (Dixon and Tyree 1984). Much like stem hygrometers, other in situ sensors embedded in the stems or trunks include those that measure the osmotic potential of the xylem tissue and calibrated to stem water potential (Meron et al. 2015). The osmotic potential sensor requires proper fluidic contact between the sensor and the plant tissue, as well has long transients (order hours) associated with the measurement.

✉ Vinay Pagay
vinay.pagay@adelaide.edu.au

[1] School of Agriculture, Food and Wine, Waite Research Institute, The University of Adelaide, PMB 1, Glen Osmond, Adelaide, SA 5064, Australia

Tensiometers measure the water potential of an external matrix by equilibrating an internal, constant volume of water whose hydrostatic pressure is taken as the negative of the external water potential. Tensiometers were originally developed for measurement of soil matric potential (Richards 1942) and have been used for irrigation scheduling of crops (Cormier et al. 2020). Based on this principle, Pagay et al. (2014) developed MEMS-based tensiometers, so-called 'microtensiometers' (MT), for rapid measurements of the water potential of an external matrix. The MTs were previously shown to operate reliably down to below − 10 MPa with short transients (equilibration or response times) of ~ 20 min. This measurement range and temporal resolution makes the sensors valuable for not only crop and soil water status monitoring, but also other contexts including meteorology, concrete curing and food processing, and other systems where the internal water status is required. Subsequent improvements on the original MT design for improved transients (faster response times) were made by Black et al. (2020). This second-generation microtensiometer was used for both in situ and ex situ measurements of water potential in a range of matrices, including foods.

This paper presents the first results of field experiments with MTs, embedded water potential sensors, in mature, irrigated grapevines in a Mediterranean climate. We compared the dynamic MT responses of plant water potential to values of leaf and stem water potentials as measured by the Scholander pressure chamber over both long-term and short-term (diurnal) periods. Our goal was to validate the use of MTs in a field context under dynamic environmental conditions.

Materials and methods

Experimental site and plant material

Two commercial vineyard blocks located in the Coonawarra region of South Australia (37.29° S, 140.83° E) were selected for the trial. One block was planted in 1988 to *Vitis vinifera* cv. Cabernet Sauvignon grafted onto Schwarzmann rootstock, while the second block was planted in 2013 to *V. vinifera* cv. Shiraz (syn. Syrah) grafted onto Teleki 5C rootstock. Both vineyards were situated within 5 km of each other and planted over the dominant 'terrarossa' soil, characterised by a distinctive red-brown, thick, clay B horizon soils overlying limestone, the depth to which is variable. In each vineyard, three adjacent vines per cultivar were selected for measurements, and additionally, the middle vine for continuous monitoring of soil and plant water status (see details below). Row and vine spacing was 2.75 m × 2.2 m. Vineyard management and integrated pest management were applied to both blocks as per convention in the region for premium wine grape production.

Irrigation was applied using a single drip line (ϕ = 21 mm) with pressure compensating emitters spaced 0.6 m apart, so each vine had approx. 3.7 drippers. The output of these emitters was 1.56 L h^{-1}. Therefore, each vine would receive approx. 5.7 L h^{-1}. Irrigation was applied weekly starting in mid-December and ranged from 3.3 mm to over 16 mm per week during the warmest period of the summer that typically included heatwaves. Irrigation decisions were made by the commercial vineyard operator that were based on a combination of historical experience, weather forecasts, and soil moisture capacitance probes where volumetric water content values were maintained over 22%. This threshold soil moisture level was based on historical experience in the vineyard block and soil type to minimise vine water stress, especially during heatwaves, which are common in the region during the growing season.

Environmental monitoring and climatic conditions

Environmental (weather) data for the vineyard blocks were obtained from the Coonawarra automatic weather station (AWS) maintained by the Australian Bureau of Meteorology (BOM), Station ID: 026091. The AWS was located approx. 200 m from the Cabernet Sauvignon vineyard and approx. 5 km from the Shiraz vineyard. Daily maximum air vapour pressure deficit (VPD) was calculated using maximum temperature and minimum relative humidity (RH) daily data. The long-term (20-year) mean January temperature (MJT) for Coonawarra is 19.3 °C and the growing degree days (GDD; base 10 °C; October–April) is 1511. The climate of the area is characterised as Mediterranean, with winter dominant rainfall and relative summer drought. Average annual rainfall for Coonawarra is approx. 569 mm (Bureau_of_Meteorology 2021). Supplemental irrigation is typically required from December until March. The elevation of the region is between 57 and 63 m above sea level.

Soil moisture measurements

Of the three sentinel adjacent vines in each cultivar/block, the middle vine was selected for continuous monitoring of soil moisture, temperature and electrical conductivity using a capacitance-based sensor (Model: Teros-12, Meter Group, Pullman, WA, USA) buried approx. 30 cm below the surface and approx. 10 cm from the trunk of the vine in the vine row. The hourly sensor data were wirelessly transmitted via telemetry to a Cloud-based server and visually displayed on a user interface (Greenbrain, Measurement Engineering Australia, Adelaide, SA, Australia).

Plant water status measurements

Leaf stomatal conductance

In each block, leaf stomatal conductance (g_s) was measured on the three sentinel vines per cultivar between 1200 and 1300 h. Measurements were performed on one fully expanded, healthy leaf per vine using an open system infrared gas analyser (IRGA; LI-6400XT, LI-COR Biosciences Inc., Lincoln, NE, USA) with a 6 cm^2 cuvette. An external LED light source (LI-6400-02B) attached to the cuvette was used at a fixed PAR value of 1500 µmol m^{-2} s^{-1} due to the sometimes variable ambient light levels. The cuvette gas flow rate was set at 400 µmol s^{-1} and reference CO_2 was set to 400 ppm. The cuvette and leaf temperatures were at ambient (uncontrolled), while cuvette relative humidity with the leaf inserted was maintained within a range of 35–55%. IRGA measurements were conducted diurnally (every 2 h between 0800 and 2000 h) on 2 days of contrasting VPDs—high VPD (February 17, 2021; max VPD ~ 6 kPa) and low VPD (January 26, 2021; max. VPD ~ 1.7 kPa)—that were typical of a Mediterranean region.

Leaf and stem water potentials

In each block, midday stem (Ψ_{stem}) and leaf water potentials (Ψ_{leaf}) were measured on adjacent mature leaves of the same shoot between the hours of 1200–1300 using a Scholander pressure chamber (Soil Moisture Equipment Corp., Santa Barbara, CA, USA). For Ψ_{stem} measurements, leaves were bagged using an opaque aluminium-lined bag for a minimum of 1 h prior to measurement to stop transpiration and allow for equilibration of water potentials between the leaf and shoot (stem). Measures of Ψ_{leaf} and Ψ_{stem} were performed on one leaf per vine from the three sentinel vines in each block/cultivar. Leaf and stem water potentials were measured diurnally on the two measurement days concurrently with IRGA measurements. The same leaf used for g_s measurement with the IRGA was used to measure Ψ_{leaf}.

Trunk water potentials

On December 12, 2020, a total of four microtensiometers (MT; FloraPulse, Davis, CA, USA) were embedded into the trunks of the grapevines, two MTs per vine per cultivar. Readers are referred to Pagay et al. (2014) for a detailed description of the theory of tensiometry, and to Black et al. (2020) for technical details of the MT sensor design, fabrication, calibration, and lab testing results (performance under controlled conditions). Two MTs (Fig. 1a) were embedded into each trunk of a woody, mature grapevine per cultivar. Sensor installation consisted of the following steps: (1) removal of bark on a flat section of the trunk; (2) removal of phloem tissue using a cork borer and spatula/blade; (3) insertion of a custom stainless steel sleeve (Fig. 1b; OD: 14 mm, ID: 9 mm) using a hammer; (4) drilling into the sleeve approx. 5 cm into the trunk (within xylem tissue) and

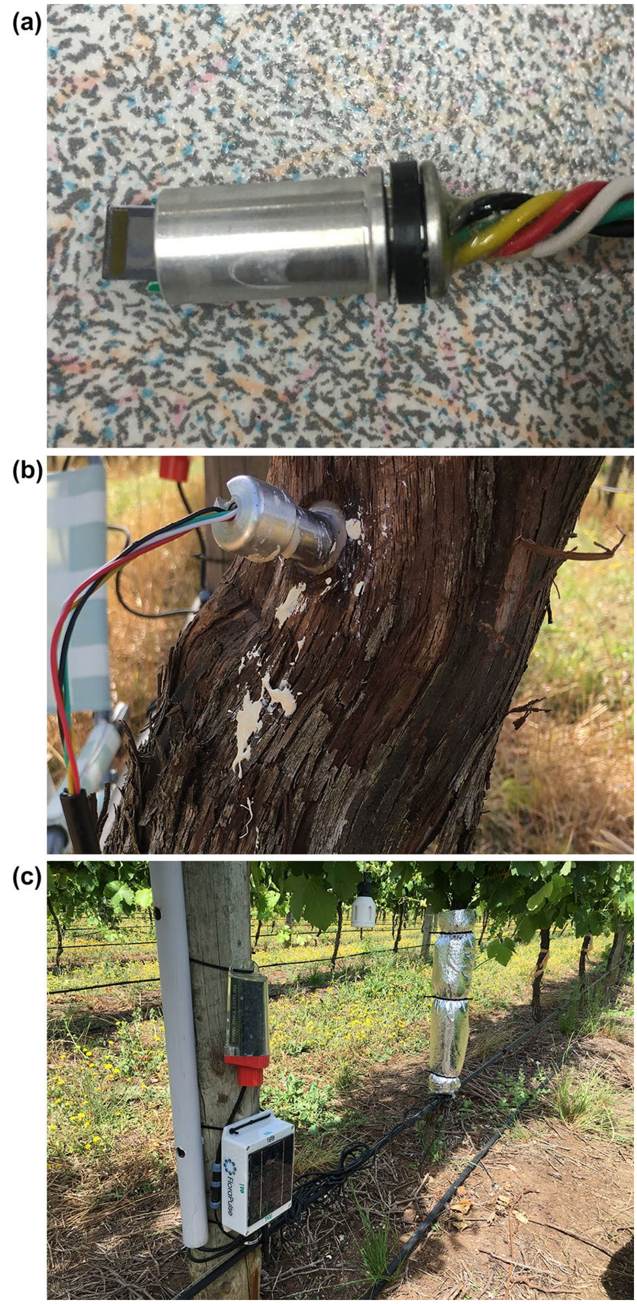

Fig. 1 **a** Close-up view of an individual microtensiometer showing the stainless steel packaging surrounding a protruding sensor chip. The tip of the chip consists of the nanoporous silicon membrane that allows for equilibration of water potentials between the exterior matrix and internal water; (**b**) MTs installed in a grapevine trunk within a stainless steel sleeve filled with kaolin mating compound; (**c**) background: MT batting and reflective film to minimise temperature effects on water potential measurements of the sensor; foreground: dataloggers and wireless transmitters of the MT (bottom unit, white box) and soil moisture sensor (top unit, red base)

Fig. 2 Seasonal patterns of (**a**) vapour pressure deficit (VPD), (**b**, **c**) total water incident (irrigation + precipitation), (**d**) soil moisture (as volumetric water content, VWC), and (**e**) trunk water potentials (Ψ_{trunk}) for Cabernet Sauvignon and Shiraz grapevines during the 2020–21 season. Approximate phenological stages shown on top of VPD graph: *FL* = flowering; *BC* = bunch closure; *V* = veraison; *PH* = approx. one week pre-harvest

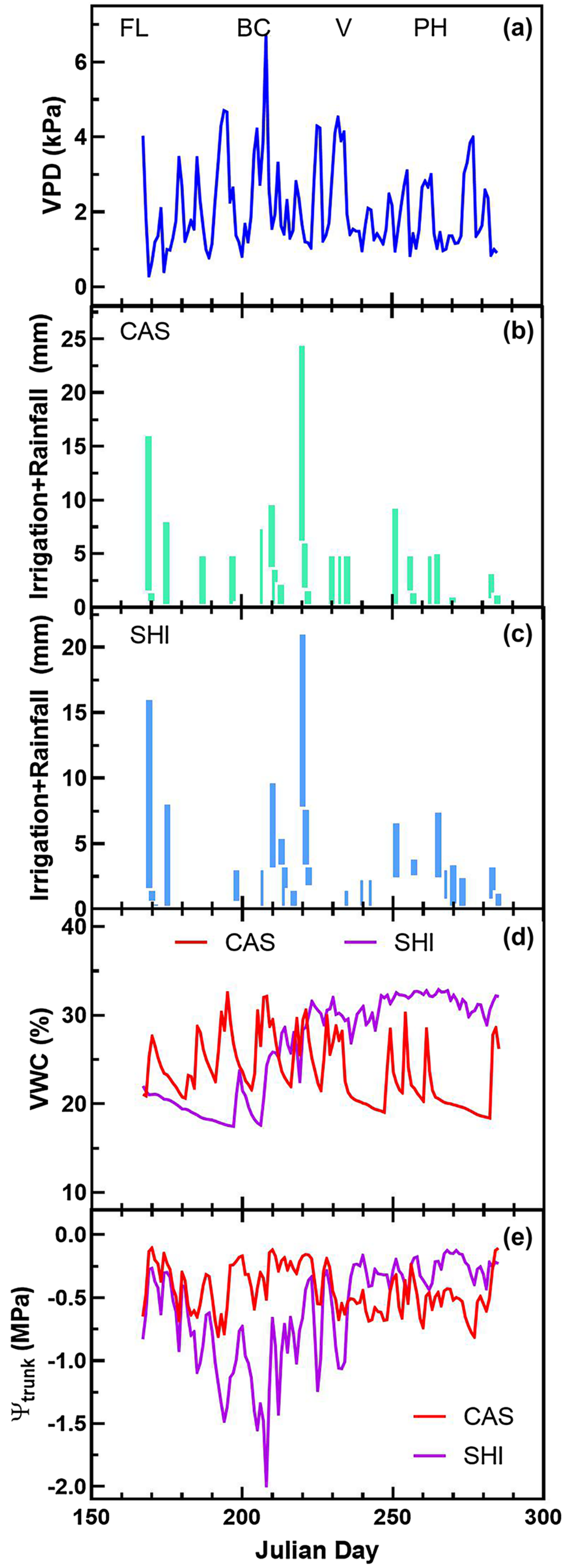

removing tissue; (5) filling the cavity with a kaolin-based mating compound; (6) inserting the hydrated MT into the mating compound; (7) placing a stainless steel cap to close the sleeve; (8) covering the sleeve exterior at the trunk with silicone to ensure air and water proofing; (9) wrapping plastic film around the sensor followed by a 25-mm-thick foam batting with reflective aluminium film to minimise exterior temperature fluctuations to the sensors (Fig. 1c). The sensors equilibrated with the vine (through the mating compound) within 2 days of installation. The MT data of trunk water potential (Ψ_{trunk}; value averaged for both sensors) were obtained every 20 min wirelessly transmitted via telemetry to a Cloud-based server (Amazon Web Services, USA) and visually displayed on a user interface (FloraPulse, Davis, CA, USA).

Statistical analyses

Time-lagged cross-correlation (TLCC) analysis was used in MATLAB programing software (v.9.8.0, R2020a, The MathWorks, Inc., Natick, MA, USA) to analyse the continuous (20-min interval) data of VPD and Ψ_{trunk} over the course of 2 days with contrasting VPDs: January 26, 2021 (low-VPD day; daily max. VPD ~ 1.6 kPa) and February 17, 2021 (high-VPD day; daily max. VPD ~ 6.7 kPa). TLCC analysis involves determining the correlations between two time series datasets that are shifted in time (Chatfield and Xing 2019), and repeatedly calculating Pearson Product Moment Correlation (cross-correlation) Coefficient (XCC) after each shift (Cheong 2020). Resulting 'offset' values, which when selected at the highest normalised XCC in the series, indicate the time shift (lag or advancement) of a particular time series compared to the other. Time shifts were selected such that they aligned with the VPD and Ψ_{trunk} measurement interval of 20 min; therefore, each offset represented 20 min.

Results

Seasonal patterns

Seasonal patterns of environmental conditions (VPD, rainfall + irrigation), soil moisture, and vine water status (Ψ_{trunk}), as measured by the microtensiometers, are shown in Fig. 2. In general, soil moisture levels correlated strongly to water incident in both vineyard, and in many cases inversely with

VPD. Microtensiometer responses (Ψ_{trunk}) reflected both soil moisture and atmospheric demand. Under high-VPD conditions, e.g. Julian Day (JD) 208 when the maximum VPD was approx. 6.7 kPa, Ψ_{trunk} values dropped by 0.2 and 0.5 MPa in Cabernet and Shiraz grapevines, respectively, despite stable or even higher soil moisture levels. Based on linear regression modelling using the same dataset to predict Ψ_{trunk} from VWC and VPD, the following relationships were obtained for CAS and SHI ($n = 119$):

$$\Psi_{trunk,CAS} = -0.983 - (0.109 \times VPD) + (0.033 \times VWC)\ (P < 0.0001)$$

$$\Psi_{trunk,SHI} = -1.187 - (0.212 \times VPD) + (0.039 \times VWC)\ (P < 0.0001)$$

The model results indicate that, while soil moisture has a similar influence on Ψ_{trunk} in both cultivars, Shiraz was more sensitive to VPD than Cabernet Sauvignon.

Seasonal courses of pre-dawn (leaf), stem and trunk water potentials are shown in Fig. 3 for Shiraz and Cabernet grapevines. In Shiraz, Ψ_{pd} values showed a declining trend over the season from JD 167, coinciding with the fruit set phenological stage until bunch closure (JD 196) followed by a recovery until harvest (Fig. 3a). This trend was matched by both Ψ_{trunk} and Ψ_{stem} albeit at lower absolute values of water potential. The lowest value of Ψ_{trunk} was observed around bunch closure at approx. −0.7 MPa. For Cabernet, the Ψ_{pd} value remained relatively stable until veraison (JD 261) when the value dropped from −0.2 MPa to −0.5 MPa by harvest (Fig. 3b). This was matched by a continually declining Ψ_{stem}, which reached a minimum of −0.9 MPa by harvest. Interestingly, the trend in Ψ_{trunk} appeared to remain fairly stable until JD 260 and then stabilised in the post-veraison period.

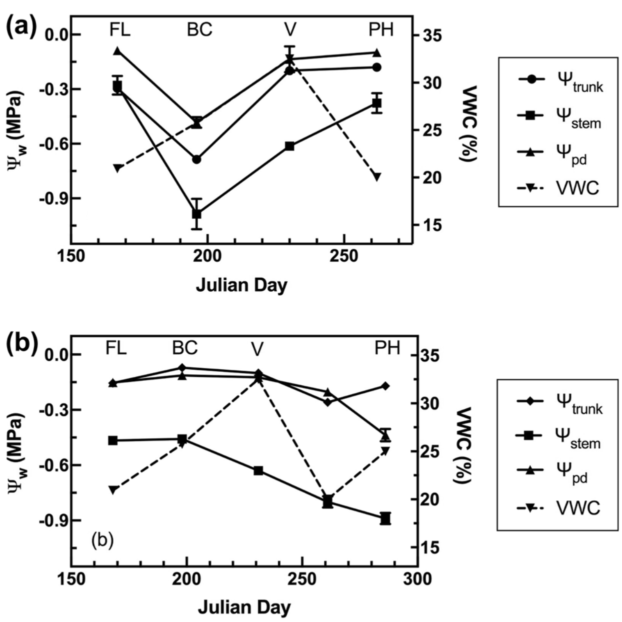

Fig. 3 Seasonal patterns of trunk (Ψ_{trunk}), stem (Ψ_{stem}), pre-dawn leaf (Ψ_{pd}) water potentials, and soil volumetric water content for (**a**) Shiraz and (**b**) Cabernet Sauvignon grapevines during the 2020–21 season. Data shown are for a single measurement vine per cultivar in which the pair of MTs was installed. Approximate phenological stages shown on top of each graph: *FL* = flowering; *BC* = bunch closure; *V* = veraison; *PH* = approx. 1 week pre-harvest

Diurnal patterns of environment and vine water status

Measurements of environmental conditions and vine water status were made over the course of 2 days, one with high vapour pressure deficit (VPD) and the other with low VPD, during the 2020–21 growing season from 0800 to 2000 h. The low-VPD day, January 26, 2021, was characterised by sunny and cool conditions, with the daily maximum temperature reaching just over 23 °C with a maximum VPD of 1.7 kPa at around 1400 h (Fig. 4a, g). On the high-VPD day, February 17, 2021, maximum daily temperature was nearly 37 °C and maximum VPD was approx. 6.0 kPa (Fig. 4d, j). The average soil volumetric water content (VWC) on the two measurement days were 24.0% and 30.6% on January 26 and February 17, respectively, in Shiraz; in Cabernet Sauvignon the VWC values were 28.3% and 30.3% on January 26 and February 17, respectively.

Under low-VPD (~ 1.7 kPa) conditions, Shiraz grapevines had Ψ_{trunk}, Ψ_{stem}, and Ψ_{leaf} daily average minimum values of −0.66, −0.96, and −1.30 MPa, respectively (Fig. 4b). Under high-VPD (~ 6 kPa) conditions, Shiraz grapevines dropped their Ψ_{trunk}, Ψ_{stem} and Ψ_{leaf} values to −1.1, −0.7, −1.5 MPa, respectively (Fig. 4e), which were considerably lower than during the low-VPD day. Under high-VPD conditions in both cultivars, patterns of plant water potential (Ψ_w) early in the day were similar to the patterns observed during the low-VPD day; the values of Ψ_w followed the expected order of $\Psi_{trunk} > \Psi_{stem} > \Psi_{leaf}$ during the morning. However, a distinct shift in the pattern of Ψ_{trunk} was observed after approx. 1400 h: Ψ_{trunk} dropped below Ψ_{stem}, reaching a minimum of −1.06 MPa around 1800 h, matching values observed for Ψ_{leaf}. In comparison, Ψ_{stem} at the same time (1800 h) was −0.47 MPa. There was a noticeable recovery (increase) in Ψ_{trunk} that started soon after 1800 h, matching the values of Ψ_{leaf} during this period late in the day (1800 h–2000 h). Under the same (high VPD) conditions, patterns of Cabernet Sauvignon Ψ_w were similar to that of Shiraz. Cabernet had large differences between Ψ_{trunk}, Ψ_{stem} and Ψ_{leaf} early in the day, and these reached their minimum values of − 0.67, − 0.76, and − 1.5 MPa, respectively, between 1400 and 1600 h (Fig. 4k). Much like Shiraz under similar (high VPD) conditions, there was a distinct crossing over of Ψ_{trunk}

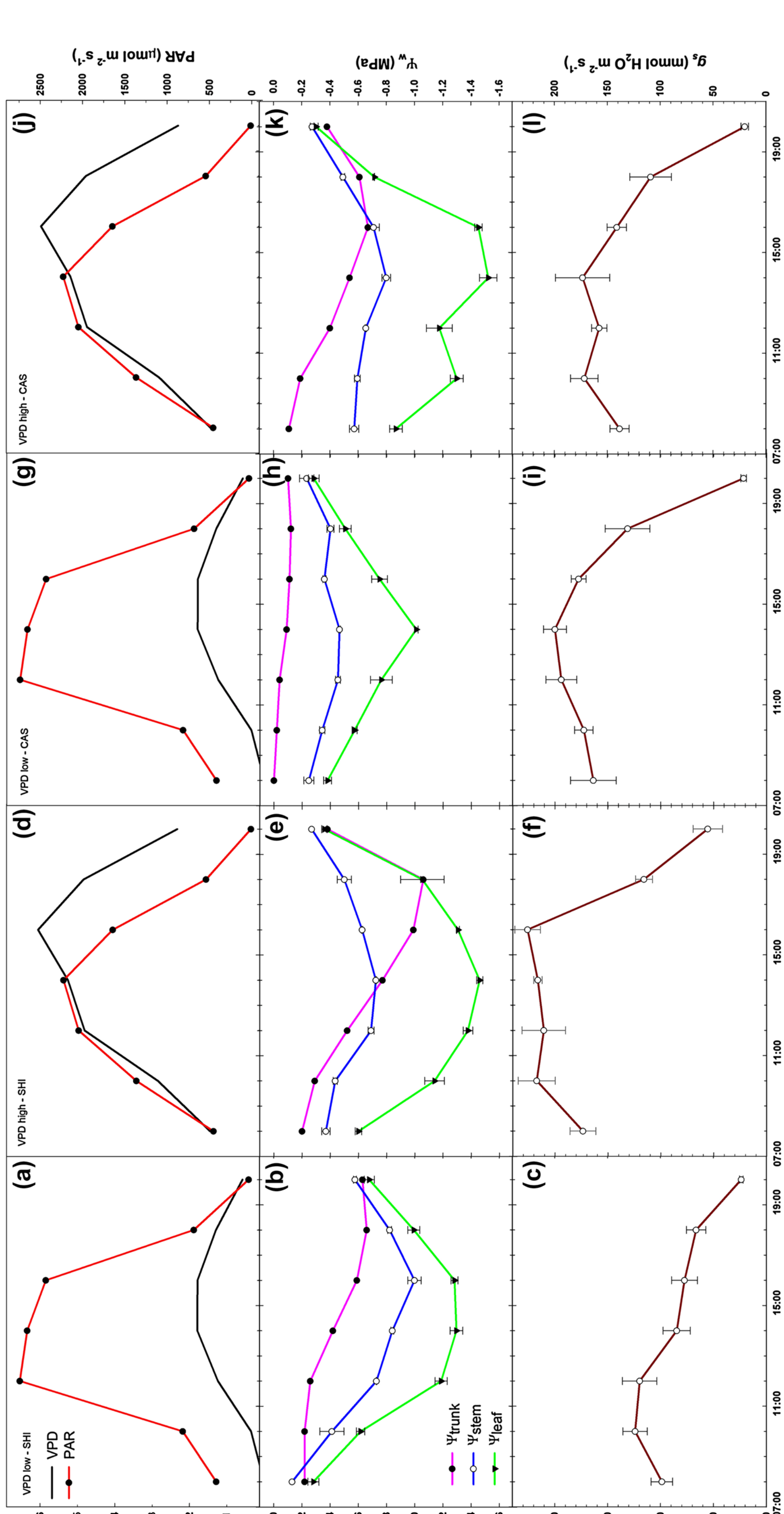

Fig. 4 Diurnal patterns of VPD, PAR, trunk (Ψ_{trunk}), stem (Ψ_{stem}), leaf (Ψ_{leaf}) water potentials, and leaf stomatal conductance (g_s) on low- and high-VPD days for Shiraz (SHI) and Cabernet Sauvignon (CAS) grapevines

and Ψ_{stem} around 1600 h; Ψ_{trunk} dropped to values below Ψ_{stem}, remaining in this position until the end of the day.

Leaf stomatal conductance (g_s) was measured concurrently with Ψ_w measurements, and on the same leaf used to measure Ψ_{leaf}. Patterns of g_s mirrored Ψ_w in both cultivars and across both measurement days under contrasting environmental conditions. In Shiraz, average g_s values were highest early in the day, peaking around 124 mmol H_2O m^{-2} s^{-1} at 1000 h under low-VPD conditions, and considerably higher around 235 mmol H_2O m^{-2} s^{-1} also at 1000 h under high-VPD conditions (Fig. 4c,d). Under high-VPD conditions, however, there was a precipitous decline in g_s after 1600 h down to similar values observed under low-VPD conditions by late day (2000 h).

Relationships between leaf, stem and trunk water potentials

Correlation analysis between various vine water potential metrics was performed to validate the Ψ_{trunk} data from the microtensiometers versus the pressure chamber-derived established metrics, Ψ_{leaf} and Ψ_{stem}. To search for robust relationships between water potential metrics for the individual cultivars, linear regression analysis was done for the combined dataset of both cultivars (Fig. 5). For Ψ_{trunk} vs. Ψ_{leaf} (Fig. 5a), the slope was approx. 0.4 ($R^2=0.21$), while for Ψ_{trunk} vs. Ψ_{stem} (Fig. 5b), the slope was higher at approx. 0.95 with higher correlation coefficients ($R^2=0.45$) and a greater agreement between the two metrics compared to Ψ_{trunk} vs. Ψ_{leaf} as indicated by the slope similarity to the 1:1 line.

Trunk water potential sensitivity to VPD

The relationships between VPD and Ψ_{trunk} for Cabernet and Shiraz for the period December 14, 2020 to February 10, 2021 (0600–2000 h) are presented in Fig. 6. There was a significant difference between cultivars in the sensitivity of vine water status to VPD (as indicated by the slopes of the regression lines) during the 2-month peak summer period. Shiraz was more sensitive than Cabernet to changes in atmospheric conditions, dropping its Ψ_{trunk} by approx. 0.17 MPa kPa^{-1}. In comparison, Cabernet reduced its Ψ_{trunk} by approx. 0.07 MPa kPa^{-1}.

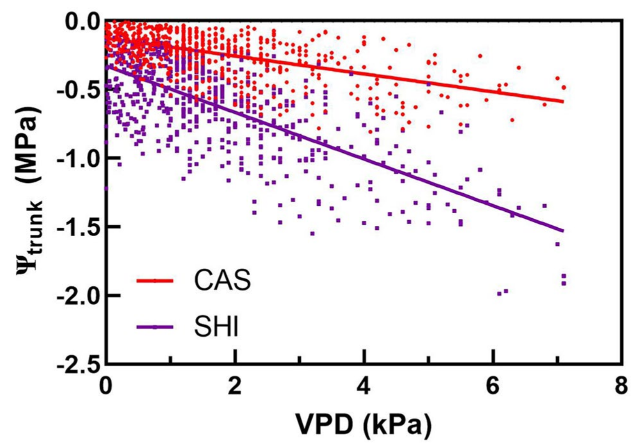

Fig. 6 Linear regression analysis of VPD vs. Ψ_{trunk} of Shiraz and Cabernet Sauvignon grapevines over the measurement period. Regression equations: Shiraz: $\Psi_{trunk}=-0.3272–0.1696*VPD$, $R^2=0.51$; Cabernet Sauvignon: $\Psi_{trunk}=-0.1247–0.065*VPD$, $R^2=0.33$. P value for differences between the slopes: <0.001

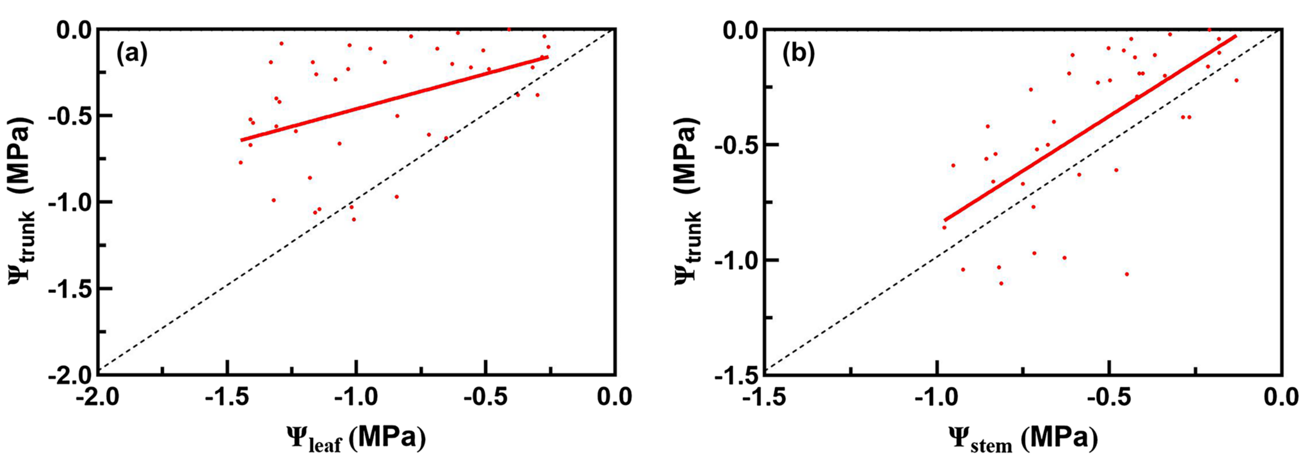

Fig. 5 Correlation analysis between trunk water potential (Ψ_{trunk}) and (**a**) leaf water potential (Ψ_{leaf}) and (**b**) stem (Ψ_{stem}) water potentials for both cultivars combined (slopes of individual cultivar regressions not significantly different). Regression equations: $\Psi_{trunk}=(\Psi_{leaf}*0.4072)-0.0531$, $R^2=0.21$ ($P=0.0022$); $\Psi_{trunk}=(\Psi_{stem}*0.9505)+0.1003$, $R^2=0.45$ ($P<0.0001$). Diagonal dotted line represents 1:1 line

Time-lagged cross-correlation analysis (TLCC) was used to analyse the time series datasets of VPD and Ψ_{trunk} across 2 days with contrasting environmental conditions or VPDs. Under low-VPD conditions (January 26, 2021; VPD ~ 1.7 kPa), TLCC analysis between VPD and Ψ_{trunk} revealed that CAS had the minimum Pearson Product Moment (normalised cross-correlation) coefficient of −180 min indicating that Ψ_{trunk} lagged VPD by 180 min. under similar (low VPD) conditions, Shiraz Ψ_{trunk} lagged VPD by 220 min. On the high-VPD day (February 17, 2021; VPD ~ 6.7 kPa), TLCC analysis revealed that CAS Ψ_{trunk} lagged VPD by 80 min while Shiraz Ψ_{trunk} lagged VPD by 120 min, both lower than the time lags observed on the low-VPD day.

Discussion

Seasonal and diurnal patterns of vine water status

In the present study, seasonal and diurnal measurements were made using MTs in Shiraz and Cabernet Sauvignon field-grown grapevines. Seasonal patterns of Ψ_{trunk} were typical of crop water potentials observed in several Mediterranean crops under supplemental irrigation (McCutchan and Shackel 1992; Williams et al. 2012) with a gradual increase of vine water stress over time. In the case of Shiraz, the steep decline observed leading up to JD 196 (Fig. 3a) resulted from a faulty valve in the sub-main irrigation line, which upon subsequent repair improved soil moisture levels and vine water status. Cabernet Ψ_{trunk} stabilised after veraison and could be related to the increase in soil moisture during this period coupled with warmer and drier conditions.

Our diurnal observations indicated that the lowest Ψ_{leaf}, Ψ_{stem}, and Ψ_{trunk} were reached around 1400 h, 1600 h and 1800 h, respectively, on low-VPD days, whereas these times were advanced on the high-VPD day, particularly for Ψ_{stem} and Ψ_{trunk}. Williams and Baeza (2007) suggested that the influence of VPD on Ψ_{leaf} decreases as soil moisture decreases. Modelling of diurnal patterns of Ψ_{leaf} predicted that the lowest values are likely to be reached around 1400 h, approx. 2 h after the highest leaf transpiration rates are reached (Katerji et al. 1986). This transient (or delay) in Ψ_{leaf} response can be attributed to the contributions of both plant tissue water and root uptake of soil moisture to the transpiration stream. These modelled patterns compare favourably with those obtained from lysimeters; maximum transpiration rates were reached between 1200 and 1400 h (Williams et al., 2012). The same study found that higher vine sizes or crop factors result in not only increased transpiration rates, as expected, but also a delayed peak by as much as 2 h. Similar patterns of vine transpiration were observed in studies using sap flow and thermal dissipation sensors (Braun and Schmid 1999; Pagay and Skinner 2018). The diurnal measurements of leaf stomatal conductance (g_s) in the present study indicated that the highest values were reached in the afternoon on low-VPD days and late morning on high-VPD days. Reductions in g_s following this peak resulted in increases in Ψ_{leaf} and Ψ_{stem}, but not Ψ_{trunk}. This lack of response from Ψ_{trunk} might indicate a level of buffering of water potential in the woody organs of the plant, in this case the trunk, where xylem vessels are surrounded by parenchymal cells that can contribute water to the transpiration stream, the so-called 'capacitance effect' (Salomón et al. 2017; Waring and Running 1978).

The highest diurnal Ψ_{trunk} observed in the present study was reached in the early morning, between 0700 and 0800 h, which is consistent with another study reporting that Ψ_{stem} does not start decreasing from its maximum diurnal value until the early morning, approx. 0700 h (Cole and Pagay 2015), but in contrast to another report that Ψ_{pd} decreases from 0330 h (Carbonneau et al. 2004). The observation has implications for the timing of measurement of Ψ_{pd}, if used as a metric for crop irrigation scheduling as recommended previously (Stricevic and Caki 1997). Donovan et al. (2001) found that Ψ_{pd} and Ψ_{p} in several woody plants may not reflect Ψ_{m} even under well-watered conditions without nocturnal transpiration. This was hypothesised to be due to the accumulation of high concentrations of solutes in the leaves, although grapevines have only modest levels of osmotic adjustment compared to many other woody horticultural crops (Rodrigues et al. 1993).

The use of trunk water potential for irrigation scheduling

MTs offer yet another plant water status metric, Ψ_{trunk}, that has been shown in this study to have a different range of values compared to conventional measures of Ψ_{leaf} and Ψ_{stem}. These conventional metrics have been well characterised for irrigation scheduling and thresholds have been suggested in the literature (Deloire and Heyns 2011; Romero et al. 2010). Trunk water potential is arguably the most stable of these three metrics, integrating all the leaves of the plant in a stable tissue that is relatively unaffected by external factors as are Ψ_{leaf} and Ψ_{stem}. Our measurements of these three vine Ψ_{w} metrics indicated that, in some instances, Ψ_{trunk} tended to be nearly 1 MPa higher than Ψ_{leaf}, indicative of the high hydraulic resistances between the trunk and leaves. Previous reports have shown that the highest hydraulic resistance in this pathway lies in the leaf, representing as much as 30% of the overall resistance in the plant (Sack et al. 2003), likely due to the fewer and narrower xylem vessels in this section of the pathway compared to distal sections. We found a weak agreement between the absolute values of Ψ_{trunk} and Ψ_{leaf} and a slightly better agreement versus Ψ_{stem}. This indicates that practitioners require new thresholds of Ψ_{trunk} to use for irrigation scheduling. The Ψ_{trunk} was also susceptible to the least fluctuations diurnally, although this was only shown to be true under low-VPD conditions (Fig. 4). Its central location in the plant between the roots and leaves, as well as buffering of xylem water status (pressure potential) via capacitance from adjoining parenchymal cells and secondary xylem (Meinzer et al. 2009) would be plausible reasons for the stability of the trunk's water status. However, we observed that Ψ_{trunk} responded to changes in soil moisture (via irrigations) less rapidly than to changes in VPD (data not shown), which suggests that the trunk may be well-coupled to the leaves despite the high hydraulic resistances in the leaf petioles. A related and somewhat surprising observation was made under high-VPD conditions: we consistently observed the crossing over of the Ψ_{trunk} and Ψ_{stem} lines in the mid-afternoon (Fig. 4e, k). The lower Ψ_{trunk} value (compared to Ψ_{stem}) during warm afternoons indicates that the trunks of both cultivars were considerably more water stressed than the stems and similar to the leaves in the late afternoon. A plausible explanation for this response is that the roots may be under water stress owing to transient water deficits at the soil-root interface due to high transpiration rates under high-VPD conditions, as well a relatively significant hydraulic resistance between the trunk and stem. Pagay et al. (2016) reported that, under high-VPD conditions, low plant water potentials could result, if the capillary conductivity of soils in the rhizosphere is inadequate to support high canopy transpiration rates. Recent reports on the existence of localised positive pressures in the xylem due to a variety of factors including osmotic exudation and/or water contributed from neighbouring parenchymal cells (Schenk et al. 2020) further support the possibility that higher water potentials in the stem compared to the trunk may exist transiently and in a localised manner, particularly when transpiration rates are low. This hypothesis needs to be tested with additional experimentation.

Continuous measurements of Ψ_{trunk} using in situ microtensiometers, which were demonstrated in field-grown plants for the first time in this study, offers a convenient measurement of plant water status for irrigation scheduling. Furthermore, these in situ measurements of plant water potential provide a useful tool for physiological studies of plant hydraulics in a dynamic environment, for example, studies on the limiting water potentials of plants as well as those involving cavitation and embolism recovery dynamics. Microtensiometers are also amenable to automation, for example, to automate irrigation scheduling via a decision support system in which thresholds of Ψ_{trunk} are pre-programmed in irrigation controllers for various crop phenological stages and that also incorporate other relevant environmental parameters such as weather forecast and soil moisture data for precision irrigation. The use of published Ψ_{stem} or Ψ_{leaf} thresholds to drive irrigation decisions should be based on measurements of the specific metric for which the threshold has been developed; a translation of those values to Ψ_{trunk} would not be appropriate due to physiological, hydraulic and anatomical differences between plants. Further research is required to validate inter-sensor variation of Ψ_{trunk} within the same plant, long-term sensor performance and stability, as well as determining Ψ_{trunk} thresholds for irrigation scheduling.

Acknowledgements The author thanks the following individuals for assistance with the project: Dr Franziska Doerflinger (Plant and Food Research Australia), Dr Michael Santiago (FloraPulse), Mr Popolopoulos, Felipe Canela, and Rochelle Schlank. The project was supported by funding from Wine Australia (project: UA 1803-1.3), and in-kind support by Katnook Estate and Wynns Coonawarra Estate.

Data availability The data supporting the findings of this study are available upon request from the author.

Declarations

Conflict of interest The author declares that no conflict of interest exists.

References

Black WL, Santiago M, Zhu SY, Stroock AD (2020) Ex situ and in situ measurement of water activity with a MEMS tensiometer. Anal Chem 92:716–723

Braun P, Schmid J (1999) Sap flow measurements in grapevines (*Vitis vinifera* L.) - 1. Stem morphology and use of the heat balance method. Plant Soil 215:39–45

Bureau_of_Meteorology (2021) http://www.bom.gov.au/climate/averages/tables/cw_026091.shtml. (Date accessed: 03/04/2021). http://www.bom.gov.au/climate/averages/tables/cw_026091.shtml. (Accessed 03/04/2021)

Carbonneau A, Deloire A, Costanza P (2004) Leaf water potential meaning of different modalities of measurements. J Int Sci Vigne Vin 38:15–19

Chatfield C, Xing H (2019) The analysis of time series: an introduction with R. Chapman & Hall/CRC texts in statistical science series, Seventh edition. edn. CRC Press, Taylor & Francis Group, Boca Raton

Cole J, Pagay V (2015) Usefulness of early morning stem water potential as a sensitive indicator of water status of deficit-irrigated grapevines (*Vitis vinifera* L.). Sci Hortic-Amsterdam 191:10–14

Corell M et al (2014) Using band dendrometers in irrigation scheduling Influence of the location inside the tree and comparison with point dendrometer. AgricWater Manag 142:29–37

Deloire A, Heyns D (2011) The leaf water potentials principles, method and thresholds. Wineland Magazine technical yearbook, pp 129–131

Dixon MA, Tyree MT (1984) A new stem hygrometer, corrected for temperature gradients and calibrated against the pressure bomb. Plant Cell Environ 7:693–697

Donovan LA, Linton MJ, Richards JH (2001) Predawn plant water potential does not necessarily equilibrate with soil water potential under well-watered conditions. Oecologia 129:328–335

Ginestar C, Eastham J, Gray S, Iland P (1998) Use of sap-flow sensors to schedule vineyard irrigation. I. Effects of post-veraison water deficits on water relations, vine growth, and yield of Shiraz grapevines. Am J Enol Vitic 49:413–420

Jones HG (1999) Use of infrared thermometry for estimation of stomatal conductance as a possible aid to irrigation scheduling. Agric for Meteorol 95:139–149

McBurney T, Costigan PA (1984) Rapid oscillations in plant water potential measured with a stem psychrometer. Ann Bot-London 54:851–853

McCutchan H, Shackel KA (1992) Stem water potential as a sensitive indicator of water stress in prune trees (*Prunus domestica* L cv French). J Am Soc Hortic Sci 117:607–611

Meinzer FC, Johnson DM, Lachenbruch B, McCulloh KA, Woodruff DR (2009) Xylem hydraulic safety margins in woody plants: coordination of stomatal control of xylem tension with hydraulic capacitance. Funct Ecol 23:922–930

Meron M, Goldberg SY, Solomon-Halgoa A, Ramon G (2015) Embedded stem water potential sensor. In: Stafford (ed) Precision agriculture. Wageningen Academic Publishers, pp 527–532

Michel BE (1977) Miniature stem thermocouple hygrometer. Plant Physiol 60:645–647

Pagay V (2016) Effects of irrigation regime on canopy water use and dry matter production of 'Tempranillo' grapevines in the semi-arid climate of Southern Oregon, USA. Agric Water Manag 178:271–280

Pagay V et al (2014) A microtensiometer capable of measuring water potentials below-10 MPa. Lab Chip 14:2806–2817

Pagay V, Zufferey V, Lakso AN (2016) The influence of water stress on grapevine (*Vitis vinifera* L.) shoots in a cool, humid climate: growth, gas exchange and hydraulics. Funct Plant Biol 43:827–837

Pagay V, Skinner A (2018) Continuous *in situ* measurements of crop water stress in 'Shiraz' grapevines using a thermal diffusivity sensor. In: Herppich WB (ed) International symposium on sensing plant water status - methods and applications in horticultural science, vol 1197. Acta Hort pp 83–88

Podobnik B, Stanley HE (2008) Detrended cross-correlation analysis: a new method for analyzing two nonstationary time series. Phys Rev Lett 100

Richards LA (1942) Soil moisture tensiometer materials and construction. Soil Sci 53:241–248

Rodrigues ML et al (1993) Osmotic adjustment in water-stressed grapevine leaves in relation to carbon assimilation. Aust J Plant Physiol 20:309–321

Romero P, Fernandez-Fernandez JI, Martinez-Cutillas A (2010) Physiological thresholds for efficient regulated deficit irrigation management in winegrapes grown under semiarid conditions. Am J Enol Vitic 61:300–312

Sack L, Cowan PD, Jaikumar N, Holbrook NM (2003) The "hydrology" of leaves: co-ordination of structure and function in temperate woody species. Plant Cell Environ 26:1343–1356

Scalisi A, Bresilla K, Grilo F (2017) Continuous determination of fruit tree water-status by plant-based sensors. Italus Hortus 24:39–50

Schenk HJ, Jansen S, Hölttä T (2020) Positive pressure in xylem and its role in hydraulic function. New Phytol 230:27–45

Scholander PF, Hammel HT, Bradstreet ED, Hemmingsen EA (1965) Sap pressure in vascular plants: negative hydrostatic pressure can be measured in plants. Science 148:339–346

Shackel K (2011) A plant-based approach to deficit irrigation in trees and vines. HortScience 46:173–177

Stricevic R, Caki E (1997) Relationships between available soil water and indicators of plant water status of sweet sorghum to be applied in irrigation scheduling. Irrig Sci 18:17–21

Waring RH, Running SW (1978) Sapwood water storage: its contribution to transpiration and effect upon water conductance through the stems of old-growth Douglas fir. Plant Cell Environ 1:131–140

Williams LE, Baeza P (2007) Relationships among ambient temperature and vapor pressure deficit and leaf and stem water potentials of fully irrigated, field-grown grapevines. Am J Enol Vitic 58:173–181

Williams LE, Baeza P, Vaughn P (2012) Midday measurements of leaf water potential and stomatal conductance are highly correlated with daily water use of thompson seedless grapevines. Irrig Sci 30:201–212